

Site-Specific Replacement of Y₃₅₆ with 3,4-Dihydroxyphenylalanine in the β₂ Subunit of *E. coli* Ribonucleotide Reductase

Mohammad R. Seyedsayamdost[†] and JoAnne Stubbe^{*†‡}

Departments of Chemistry and Biology, Massachusetts Institute of Technology, 77 Massachusetts Avenue, Cambridge, Massachusetts 02139-4307

Received November 15, 2005; E-mail: stubbe@mit.edu

Ribonucleotide reductases (RNRs) catalyze the conversion of nucleotides to deoxynucleotides in all organisms, providing the monomeric precursors required for DNA replication and repair.¹ The class Ia RNR in *E. coli* is composed of a complex of two homodimeric subunits: α₂ and β₂. α₂ houses the site for nucleotide reduction and additional binding sites for dNTP and ATP/dATP effectors that control substrate specificity and turnover rates. β₂ contains the diferric-tyrosyl radical cofactor (Y₁₂₂•), essential for initiation of the radical-dependent reduction process. The mechanism of nucleotide reduction within α₂ is thought to be initiated by hydrogen atom abstraction from the nucleotide by a transiently generated thiyl radical (C₄₃₉•).² The mechanism of radical propagation, however, how Y₁₂₂• in β₂ generates this transient C₄₃₉• in α₂ over a distance of 35 Å, remains unresolved.³ The current proposal for the radical propagation pathway, shown in Figure 1, is based on a docking model of α₂ and β₂ structures and involves aromatic amino acid residues.^{3a} Evidence in support of the long distance and the docking model has recently been obtained by pulsed EPR methods.⁴ Evidence has also been obtained for the role of Y₃₅₆ in the pathway by site-specific incorporation of F_nYs (*n* = 1–4)⁵ and 3-NO₂-Y⁶ into this position by intein technology. In this communication, we report the semi-synthesis of β₂, where Y₃₅₆ has been replaced with 3,4-dihydroxyphenylalanine (DOPA).⁷ This construct (DOPA₃₅₆-β₂) is then used to trap the DOPA radical intermediate (DOPA•) in the presence of α₂, substrate (CDP or GDP), and effector (ATP, TTP); it is also used as a reporter of conformational gating between α₂ and β₂.⁸

The choice of DOPA as a probe was based on its reduction potential of 570 mV (vs NHE), 260 mV lower than Y at pH 7.0,¹⁰ suggesting that it could be readily oxidized and serve as a radical trap during the propagation step. However, a DOPA• would be unlikely to oxidize Y₇₃₁ in α₂, thus preventing nucleotide reduction. Activity assays of DOPA₃₅₆-β₂ with α₂, CDP, and ATP revealed no deoxynucleotide formation; that is, the rate was 10⁴-fold less than that of intein-generated wt-β₂,¹¹ consistent with this proposal. To examine this model further, stopped flow (SF) UV–vis experiments were carried out. DOPA₃₅₆-β₂ and GDP in one syringe were rapidly mixed with α₂ and effector TTP from a second syringe.¹² The reaction was monitored at 305 nm (the reported λ_{max} of DOPA• with ε = 12 000 M⁻¹ cm⁻¹) and at 410 nm (the λ_{max} of Y₁₂₂• with ε = 3700 M⁻¹ cm⁻¹).¹³ As shown in Figure 2A, Y₁₂₂• (red) disappears, while a feature at 305 nm, proposed to be the DOPA• (blue), grows in with similar kinetics. Analysis of the kinetic traces in the reaction with GDP/TTP reveals a fast phase, followed by a slow phase that can be fit to two single exponentials (Table 1, Supporting Information). A point-by-point analysis of the new species revealed the spectrum shown in Figure 2B. This spectrum is identical to that previously reported^{13a} for a DOPA•, except that

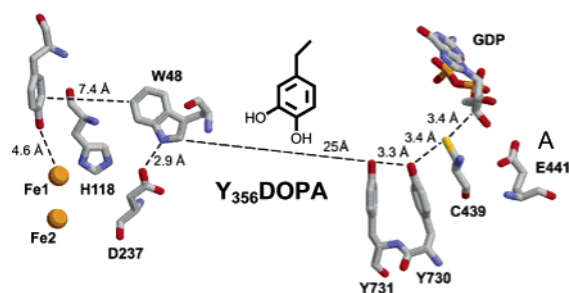


Figure 1. Proposed pathway for radical initiation based on the α₂/β₂ docking model with DOPA inserted in place of Y₃₅₆. The distance between W48 and Y731 is based on the docking model.^{3a} Other distances are from structures of α₂^{3a} and β₂⁹.

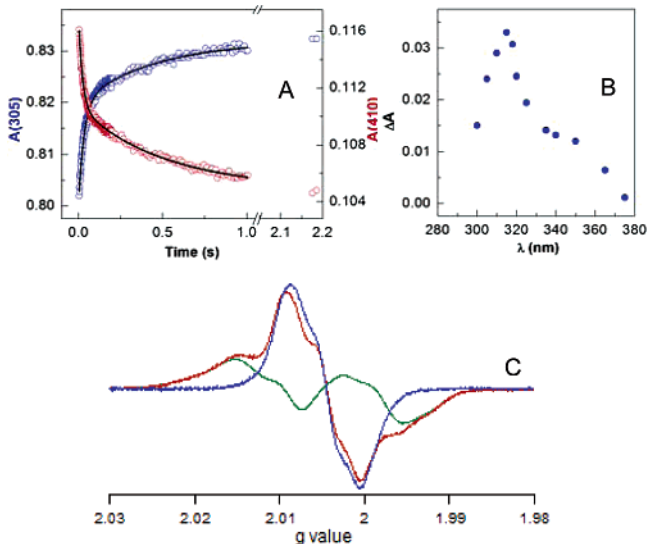


Figure 2. (A) Kinetics of DOPA• formation (blue) and Y₁₂₂• disappearance (red) with GDP/TTP. Black lines indicate fits to the data. (B) Point-by-point reconstruction of the DOPA• spectrum. (C) EPR spectrum of the radicals observed by reacting DOPA₃₅₆-β₂ with α₂/GDP/TTP (red); contribution to the spectrum by unreacted Y₁₂₂• (green) and subtraction of Y₁₂₂•, yielding the DOPA• spectrum (blue).

it is red-shifted by 10 nm, suggesting an effect of the protein environment at the α₂/β₂ interface.

To provide further support for the structure associated with the 315 nm feature, an experiment under similar conditions to those described above was carried out. The sample was frozen at 5 s and examined by 9 GHz EPR spectroscopy;^{14a} the resulting spectrum is shown in Figure 2C and consists of contributions from unreacted Y₁₂₂• and a newly formed radical (red). Subtraction of 0.53 equiv of Y₁₂₂• (green) gives rise to a spectrum identical to that of a DOPA• (blue).^{14b,c} Together, the data in Figure 2 provide compelling

[†] Department of Chemistry.

[‡] Department of Biology.

Table 1. Characterization of DOPA₃₅₆-β2/α2 with Various Substrate/Effector Pairs by SF UV-vis and EPR

Substrate/ Effector	RNR Subunits	1 st Phase ^a		2 nd Phase ^a		3 rd Phase ^a		% total Y ₁₂₂ [•] trapped as DOPA [•] by SF	% total Y ₁₂₂ [•] trapped as DOPA [•] by EPR ^c
		k _{obs} (s ⁻¹), Amp (%) ^b	k _{obs} (s ⁻¹), Amp (%) ^b	k _{obs} (s ⁻¹), Amp (%) ^b	k _{obs} (s ⁻¹), Amp (%) ^b	k _{obs} (s ⁻¹), Amp (%) ^b	k _{obs} (s ⁻¹), Amp (%) ^b		
GDP/TTP	DOPA-β2/α2	32 ± 5, 31 ± 2	1.7 ± 0.05, 23 ± 1	---	---	---	---	54	47
GDP	DOPA-β2/α2	13 ± 2.5, 26 ± 2	0.8 ± 0.09, 13 ± 1	---	---	---	---	39	47
TTP	DOPA-β2/α2	0.4 ± 0.01, 14 ± 1	---	---	---	---	---	14	6
CDP/ATP	DOPA-β2/α2	38 ± 0.5, 21 ± 1	6.8 ± 0.1, 17 ± 0.6	0.7 ± 0.12, 9 ± 2	---	---	---	47	49
CDP/TTP	DOPA-β2/α2	43 ± 2.5, 22 ± 2	4.2 ± 0.6, 14 ± 1	0.7 ± 0.01, 10 ± 0.4	---	---	---	46	nd ^d
CDP	DOPA-β2/α2	28 ± 0.3, 9 ± 2	6.8 ± 0.6, 21 ± 0.3	0.5 ± 0.1, 11 ± 1.7	---	---	---	39	48
---	DOPA-β2	---	---	---	---	---	---	---	---
---	DOPA-β2/α2	---	---	---	---	---	---	---	---
CDP/ATP	met-DOPA-β2/α2	---	---	---	---	---	---	---	---

^a The rate constants reported are the average of those measured at 410 nm for Y₁₂₂[•] loss and at 305 nm for DOPA[•] formation. In the case of DOPA[•], the ϵ was calculated using the following:^{13a} $\epsilon(305) = \epsilon(315) \times (\text{Abs}_{305}/\text{Abs}_{315})$. ^b Amp = amplitude; the amount of Y₁₂₂[•] trapped in each kinetic phase is indicated as a % of total initial Y₁₂₂[•] in SF and EPR experiments. ^c EPR quantitation was carried out using Cu^{II} as standard. ^d nd = not determined.

evidence for the first trapping of a redox-active residue in the radical propagation pathway.

Two additional experiments were carried out to examine the affect of substrate, GDP, and effector, TTP, individually. In the former case, the kinetics are similar to that observed in the GDP/TTP case (Table 1, 2nd row). In the latter case, a single, slow kinetic phase is observed (Table 1, 3rd row).

Several controls were carried out to ensure that formation of DOPA[•] is associated with the pathway for radical propagation between α2 and β2 (Table 1). In one control, DOPA₃₅₆-β2 was examined alone. In the second control, DOPA₃₅₆-β2 and α2 were rapidly mixed in the absence of substrate and effector, and in the third control, met-DOPA₃₅₆-β2 (DOPA₃₅₆-β2 with its Y₁₂₂[•] reduced to Y₁₂₂) and substrate were mixed with α2 and effector. No spectral changes were observed in any of these cases. The formation of DOPA[•] appears to be kinetically linked to Y₁₂₂[•] loss and is only triggered by the presence of substrate and/or effector.

The observed rate constants for the fast and slow phases of DOPA[•] formation may be providing insight into the radical propagation step. The rate constant for the slow phase is close to the turnover number of intein-generated wt-β2 under similar conditions. Thus DOPA[•] formation in the slow phase may be reporting directly on the conformational gating event, which has previously been postulated to be rate-determining in the reaction of non-intein wt-β2.¹⁵ We suggest that the rapid phases are substrate-mediated conformational changes that place ~50% of the α2/β2 complex into an active conformation for turnover. Because of the enhanced sensitivity of DOPA to oxidation, the radical perhaps equilibrates within the aromatic residues of β2 and gets trapped at 356. With effector alone, however, after 1 s, only ~10% of the complex is in its active form. These results suggest that substrate plays a major role in conformational gating. This interpretation is consistent with experiments carried out on CDP/ATP, CDP/TTP, and CDP alone, where regardless of the nature or presence of the effector, similar kinetics of DOPA[•] formation are observed (Table 1).

One puzzling observation remains unexplained: in all substrate/effector reactions examined, only ~50% of total Y₁₂₂[•] is consumed. While at present we do not understand this result, it is in line with results from a mechanism-based inhibitor and pulsed EPR studies,⁴ and pre-steady-state experiments monitoring dCDP¹⁵ and disulfide bond¹⁶ formation in α2, all of which suggest that the active RNR complex is asymmetric.

The studies reported in this contribution have provided the first kinetically competent trapping of a redox-active residue in the proposed radical propagation pathway. The requirement for the

presence of substrate and/or effector strongly implies pathway dependence. The kinetic data provide the first information about rate constants for conformational changes triggered by substrate and/or effector binding. Further studies will establish if these changes also provide insight into the asymmetry within the active RNR complex.

Acknowledgment. We would like to thank Prof. Daniel G. Nocera and Steven Y. Reece for helpful discussions, and John H. Robblee for help with EPR data analysis. We also acknowledge support from NIH Grant GM29595.

Supporting Information Available: RP-HPLC profile and MALDI-TOF MS of DOPA-22mer peptide, SDS-PAGE gel of purified DOPA₃₅₆-β2, and SF UV-vis traces of reactions in Table 1. This material is available free of charge via the Internet at <http://pubs.acs.org>.

References

- Jordan, A.; Reichard, P. *Annu. Rev. Biochem.* **1998**, *67*, 71–98.
- Stubbe, J.; van der Donk, W. *Chem. Rev.* **1998**, *98*, 705–762.
- (a) Uhlir, U.; Eklund, H. *Nature* **1994**, *370*, 533–539. (b) Stubbe, J.; Nocera, D. G.; Yee, C. S.; Chang, M. C. Y. *Chem. Rev.* **2003**, *103*, 2167–2201.
- Bennati, M.; Robblee, J. H.; Mugnaini, V.; Stubbe, J.; Freed, J. H.; Borbat, P. *J. Am. Chem. Soc.* **2005**, *127*, 15014–15015.
- (a) Seyedsayamdost, M. R.; Reece, S. Y.; Nocera, D. G.; Stubbe, J. *J. Am. Chem. Soc.* **2006**, in press. (b) Seyedsayamdost, M. R.; Yee, C. S.; Reece, S. Y.; Nocera, D. G.; Stubbe, J. *J. Am. Chem. Soc.* **2006**, in press.
- Yee, C. S.; Seyedsayamdost, M. R.; Chang, M. C. Y.; Nocera, D. G.; Stubbe, J. *Biochemistry* **2003**, *42*, 14541–14552.
- See Supporting Information for semi-synthesis of DOPA₃₅₆-β2.
- Zlateva, T.; Quaroni, L.; Que, L.; Stankovich, M. T. *J. Biol. Chem.* **2004**, *279*, 18742–18747. Here, conformational changes in the *E. coli* RNR complex were investigated by measuring the reduction potential of Y₁₂₂[•] in the presence of different substrates and effectors.
- Högbom, M.; Galander, M.; Andersson, M.; Kolberg, M.; Hofbauer, W.; Lassman, G.; Nordlund, P.; Lendzian, F. *Proc. Natl. Acad. Sci. U.S.A.* **2003**, *100*, 3209–3214.
- Jovanovic, S. J.; Steenken, S.; Tosic, M.; Marjanovic, B.; Simic, M. G. *J. Am. Chem. Soc.* **1994**, *116*, 4846–4851.
- Intein-generated wt-β2 has the mutations V353G/S354C not present in wt-β2. The activity assays were carried out as described in ref 6. The specific activity of [¹⁴C]-CDP was 8150 cpm/nmol. The radical content of DOPA-β2 was ~0.3/dimer, similar to that of intein-generated wt-β2.
- DOPA₃₅₆-β2 (45 μM) and GDP (2 mM) were rapidly mixed at 25 °C in a 1:1 ratio with pre-reduced α2 (45 μM) and TTP (200 μM).
- (a) Craw, M.; Chedekel, M. R.; Truscott, T. G.; Land, E. J. *Photochem. Photobiol.* **1984**, *39*, 155–159. (b) Bollinger, J. M., Jr.; Tong, W. H.; Ravi, N.; Huynh, B. H.; Edmondson, D. E.; Stubbe, J. *Methods Enzymol.* **1995**, *258*, 278–303.
- (a) A sample containing 25 μM DOPA₃₅₆-β2, 25 μM pre-reduced α2, 1 mM GDP, and 100 μM TTP was incubated at 25 °C and hand-quenched at approximately 5 s by freezing in liquid N₂. Stoichiometric spin was recovered within experimental error. (b) Sealy, R. C.; Hyde, J. S.; Felix, C. C. *Science* **1982**, *217*, 545–547. (c) Chen, Y. R.; Chen, C. L.; Chen, W.; Zweier, J. L.; Augusto, O.; Radi, R.; Mason, R. P. *J. Biol. Chem.* **2004**, *279*, 18054–18062.
- Ge, J.; Yu, G.; Ator, M.; Stubbe, J. *Biochemistry* **2003**, *42*, 10071–10083.
- Erickson, H. K. *Biochemistry* **2001**, *40*, 9631–9637.

JA057776Q